Design of mm-RoF system based on OFM technique with optimized OFDM modulation

Rujian Lin (林如俭)*, Xiang Chen (陈 翔), Lin Zhang (张 林), Jiajun Ye (叶家骏), Yingxiong Song (宋英雄), and Yingchun Li (李迎春)

Key Laboratory of Specialty Fiber Optics and Optical Access Networks, Shanghai University, Shanghai 200072, China

**Corresponding author: rujianlin@shu.edu.cn*

Received December 16, 2011; accepted March 14, 2012; posted online, 2011

We present the design of a novel bi-directional millimeter-wave radio-over-fiber (mm-RoF) system based on the millimeter-wave generation by optical frequency multiplication (OFM). A dual-drive Mach-Zehnder modulator is used to generate high-order optical side-modes which beat in the photo-detector, producing a 40-GHz carrier. Over 100-Mb/s orthogonal frequency division multiplexing (OFDM) modulation scheme is employed. The emphasis is on developing a mathematical model for optimizing optical modulation index to the Mach-Zehnder intensity modulator (IM) for OFDM signal with high peak-to-average power ratio which imposes a limitation on the system bit error rate (BER) performance due to the non-linearity of IM. The theoretical analysis on composite carrier to composite triple beat ratio is performed based on which extension to the system BER formula for quadrature phase shift keying/ multiple quadrature amplitude modulation (QPSK/MQAM) format is presented. The experimental proof is given in a 40-GHz RoF system at a bit rate of up to 280 Mb/s in 100-MHz bandwidth.

OCIS codes: 060.4250, 060.4510.
doi: 10.3788/CJL201239.0805007.

1 Introduction

The millimeter-wave radio-over-fiber (mm-RoF) system as an optical/wireless convergence platform has been under much investigation over the last decade. To increase the capacity of wireless networks, various international standards in the mm-band have been developed including IEEE 802.16, 802.15.3c, and P802.11ad. Due to the very limited transmission distances of millimeter waves in the air, such as 1 km at 40 GHz and 10 m at 60 GHz, a mm-network is composed of many base stations (BSs), with each serving a pico cell and is connected to the central station (CS) by an optical fiber taking advantage of its huge bandwidth and extremely low loss. Therefore, a mm-RoF system between CS and BSs should be designed in a cost-effective way that all network control functions are concentrated on CS, making BS a simple optical-mm-converter. Previous research studies focused on the photonic generation of millimeter wave in the downlink (CS to BS). However, only a few paid attention to the stability of the optically generated millimeter wave and the uplink implementation, such that many mm-RoF systems still remained as non-real-time and one-way links. Among various photonic methods currently proposed, the optical frequency multiplication (OFM) based on the self-heterodyne of high-order optical side-modes[1−6], to realize harmonic generation from low frequency microwave, is a cost-effective technique without a need for expensive optical and millimeter-wave active devices.

In the multi-level modulation schemes adopted in mm-RoF systems, orthogonal frequency division multiplexing (OFDM) has been recognized as a good signal-carrying scheme[3−6], owing to its high spectral efficiency and robustness to the linear and non-linear distortions in the fiber link. Optical OFDM has been widely discussed, but most of them are dealing with the dispersion effects and non-linear distortion tolerance in long-haul fiber transmission systems[6] in which major impairments are from the characteristics of optical fiber, such as chromatic dispersion (CD), polarization mode dispersion (PMD), self-phase modulation (SPM), and cross-phase modulation (XPM). In these cases, the prefix insertion/removal and post-digital signal procession for the OFDM signal are effective techniques to overcome system impairments. However, in short-distance cases such as the mm-RoF system and OFDM passive optical network (PON), the fiber non-linearity can be neglected. Linear impairment is the CD-induced fading of millimeter wave, while non-linear impairment is the inter-channel interference caused by the non-linearity of optical devices under the condition of high peak-to-average power ratio (PAPR) of the OFDM signal. Linear impairment has been widely discussed, whereas non-linear impairment has not been fully investigated yet.

This letter deals with the design of the 40-GHz RoF system which carries out the mm-generation by a new OFM scheme using a dual-drive Mach-Zehnder modulator (DD-MZM) and OFDM modulation on an intensity modulator (IM). The design is an inexpensive bi-directional mm-RoF/wireless link integration without using mm-oscillators.

2 Principle of millimeter wave generation by OFM

In principle, the mm-generation by OFM works in the self-heterodyne of high-order optical side-modes. This

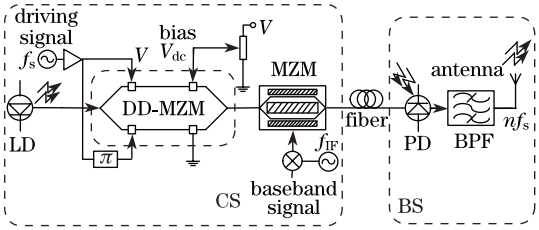

Fig. 1. OFM system with DD-MZM.

technique has been developed, whose core function block is the optical side-mode generator comprising an optical phase modulator (PM) and an optical-phase-to-intensity converter originally proposed in Ref. [1].

Alternatively, we use a DD-MZM to replace the optical PM and interferometer (MZI), as shown in Fig. 1, because optical phase modulation and optical-phase-to-intensity conversion can be carried out by just one DD-MZM. The two arms of DD-MZM are driven in a push-pull style with a large optical phase modulation index. The intensity of the injected light wave is modulated, yielding many side-modes whose amplitudes obey Bessel functions of the optical phase modulation index. After transmitting to the fiber, these optical side-modes beat in photo-detector (PD) at BS, generating a series of harmonics of the driving microwave, as shown in Fig. 2, among which any harmonic can be picked up by a specific band-pass filter (BPF). Without any periodic optical filter and tunable laser, this mm-generation solution is more cost-effective and stable than the original one.

The modulation curve of DD-MZM driven in a push-pull fashion is expressed as

$$I_o(t) = \frac{1}{4}E_c^2\left\{1+\cos\left[\pi\frac{V_{dc}}{V_\pi}+\pi\frac{2V(t)}{V_\pi}\right]\right\}, \qquad (1)$$

where I_o is the output optical intensity of DD-MZM, E_c is the amplitude of the input electrical field, V_{dc} is the DC bias voltage, V_π is the half-wave voltage of DD-MZM, $V(t) = V_p \sin\omega_s t$ is the driving voltage on one arm with amplitude V_p, and angular frequency ω_s.

Let V_{dc}=0, I_o is evenly symmetrical and can be expressed in a series with the Bessel function as

$$I_o(t) = \frac{1}{4}E_c^2\left[1+J_0(2\beta)+2\sum_{n=1}^{\infty}J_{2n}(2\beta)\cos(2n\omega_s t)\right], \quad (2)$$

where $\beta = \pi V_p/V_\pi$ is the optical phase modulation index. The output optical intensity comprises only an even order of harmonics of the driving microwave. However, if $V_{dc} = \Delta V \neq 0$, the amplitudes of the even harmonics decay as ΔV grows, while odd harmonics appear. Unexpectedly, the modulation curve of DD-MZM drifts with temperature and the large microwave driving power produces heat in DD-MZM. Therefore, the major challenge to this OFM scheme is temperature stability. We place DD-MZM in a thermo-isolation container which is automatically temperature-controlled by a semi-conductor cooling loop, resulting in 35±0.02 °C variance that ensures the stability of the generated millimeter wave.

The frequency of the generated radio frequency (RF) signal in BS can be 2n-folds the driving frequency (n=1−6), as long as the driving voltage is set sufficiently high. For system cost-effectiveness, we keep the driving frequency below 10 GHz. Therefore, for a millimeter wave generated at 40 GHz from a microwave at 5 GHz, the multiplication factor 8 is needed. The best level of driving microwave is the most important parameter of the OFM system. To maximize $J_{2n}(2\beta)$, a specific value of β is obtained. For example, for the multiplication factor 8, we set β=4.825 which corresponds to the maximal $J_8(9.65) = 0.324\,4$ and $V_p = 1.536 \times V_\pi$. For $V_\pi = 4.6$ V, the driving power to DD-MZM is 27 dBm.

To carry the base-band information, an IM is set up following the DD-MZM. The modulating signal to IM is an OFDM-modulated intermediate frequency (IF) signal. The second optical modulation should be linear to avoid inter-channel interference. The information-carrying IF side-bands exist around each harmonic carrier, as shown in Fig. 2.

3 System architecture of bi-directional ROF system based on OFM

Based on OFM using DD-MZM, a bi-directional 40-GHz RoF system is configured (Fig. 3). In the downstream, a 1 550-nm distributed feedback (DFB) laser (LD) in CS transmits light waves into DD-MZM. Two 5-GHz sinusoidal waves drive DD-MZM in a push-pull fashion to generate optical side-modes which are modulated in IM by an OFDM-modulated 2.4-GHz IF signal and then sent over a downlink fiber up to 20 km to reach PD in BS where many electrical harmonics of 5-GHz signal are generated. In this way not only a pure 40-GHz carrier, but also an OFDM-modulated 37.6-GHz lower side-band signal is generated. Both are amplified and radiated into the air via a duplexer/antenna, while the pure 40-GHz carrier is filtered and amplified as local oscillation (LO) to be used for the down-conversion in the uplink. In the upstream, an OFDM-modulated upper side-band signal at 42.4 GHz received from the air is first amplified by a low noise amplifier (LNA) and then mixed with LO, resulting in an OFDM-modulated IF signal. The amplified IF signal is sent back to CS via LD and an uplink fiber, and then recovered at PD in CS. Finally, the amplified IF signal is demodulated in an OFDM modem.

We investigated two kinds of system: real-time, bi-directional and non-real time systems. So far, most published research results on RoF systems are from non-real time experiments[1−5]. We construct a real-time 40-GHz RoF/wireless network using market-available wireless devices. Specifically, IEEE802.11n transceivers and OFDM modems are used. An 802.11n router is placed in CS,

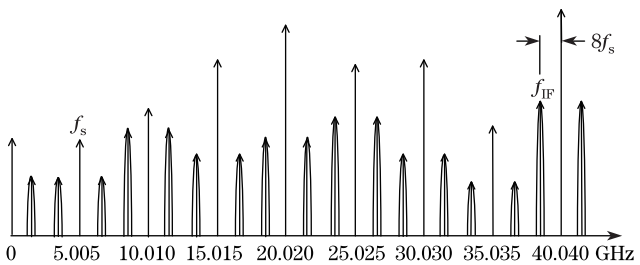

Fig. 2. Spectrum of generated RF signal in BS.

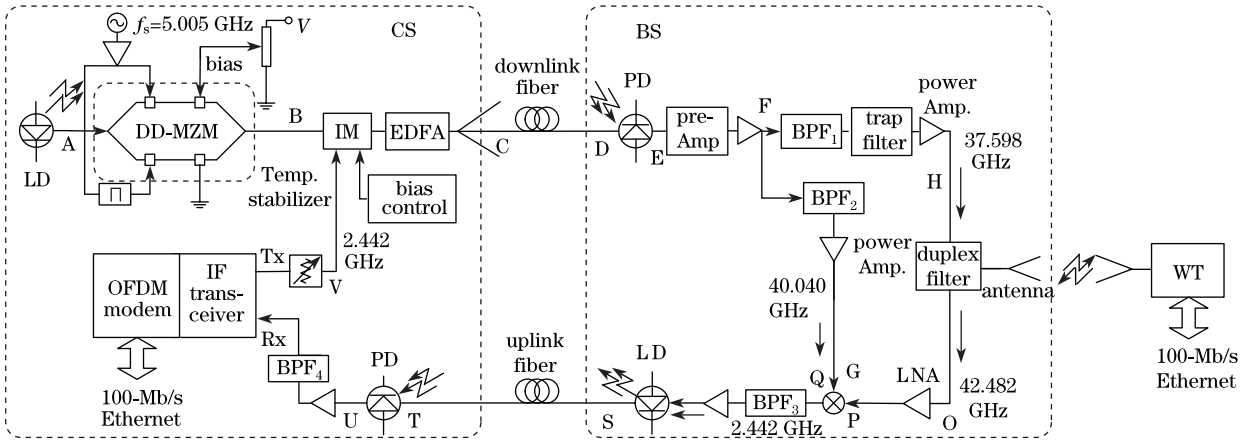

Fig. 3. Bi-directional 40-GHz RoF system based on OFM using DD-MZM.

while 802.11n NIC is placed in the wireless terminal (WT), both having a 100-Mb/s Ethernet interface. However, the burst-mode operation of 802.11n devices makes the study on optimum modulation index to IM difficult. Therefore, a one way non-real time 40-GHz RoF system is also configured using arbitrary waveform generator (TEK7211C)/digital oscilloscope (DSO80604B, Agilent) platform plus MatLab software as an offline OFDM modem.

4 Analysis on the optimal optical modulation index of $LiNbO_3$ IM

Since the OFDM signal with big PAPR is subject to the non-linear distortion in modulation, the non-linearity of the optical modulator needs to be carefully considered. The non-linearity of $LiNbO_3$ IM was investigated for multi-channel CATV signal in 90 s[7]. Since then, it has not received much attention because the two-level base-band digital transmission is not sensitive to modulator non-linearity. At present, the non-linear distortion of analog-like IF OFDM signal in $LiNbO_3$ IM should be investigated in detail because the distortion causes in-band interference[8]. In previous literatures, linearization techniques such as pre-distortion and pre-clipping have been discussed, while the degradation of the OFDM system performance caused by the in-band interference has not been evaluated which will be conducted in this letter.

An OFDM signal of N sub-carriers is expressed as

$$v(t)=\sum_{k=1}^{N}\sum_{n=-\infty}^{+\infty}A_{k,n}\mathrm{e}^{\mathrm{j}\theta_{k,n}}g(t-nTs)\mathrm{e}^{\mathrm{j}(\omega_0+2\pi k f_\mathrm{s})t}, \quad (3)$$

where ω_0 is the intermediate angular frequency, f_s and T_s are the symbol frequency and symbol period, respectively, $g(t)$ is the base-band signal waveform, and $A_{k,n}$ and $\theta_{k,n}$ are the amplitude and the phase of the kth modulation vectors, respectively, which are orthogonal, i.e. their discrete auto-correlation is

$$\begin{aligned}R_\mathrm{a}(n-m)&=\frac{1}{2}E\{A_{k,n}^{*}\mathrm{e}^{-\mathrm{j}\theta_{k,n}}A_{k,m}\mathrm{e}^{\mathrm{j}\theta_{k,m}}\}\\&=\frac{1}{2}E\{A_{k,n}^{2}\}\delta_{n,m}=\sigma_k\delta_{n,m},\end{aligned} \quad (4)$$

where E{ } represents the mathematic expectation.

The auto-correlation function of $v(t)$ is expressed as

$$\begin{aligned}R_v(t,t+\tau)&=\frac{1}{2}E\{v^{*}(t)v(t+\tau)\}=\sum_{k=1}^{N}\mathrm{e}^{\mathrm{j}(\omega_0+2\pi k f_s)\tau}\\&\cdot\sum_{m=-\infty}^{+\infty}\sigma_k^2 g(t-mT_\mathrm{s})g(t+\tau-mT_\mathrm{s}).\end{aligned}$$

Since $R_v(t,t+\tau)$ is a cyclo-stationary process at period T_s, an average over T_s is derived as

$$\begin{aligned}\overline{R_v(\tau)}&=\frac{1}{T_\mathrm{s}}\int_{-T_s/2}^{+T_s/2}R_v(t,t+\tau)\mathrm{d}t\\&=\frac{1}{T_\mathrm{s}}\sum_{k=1}^{N}\sigma_k^2\mathrm{e}^{\mathrm{j}(\omega_0+2\pi k f_\mathrm{s})\tau}\phi_{gg}(\tau),\end{aligned} \quad (5)$$

where $\phi_{gg}(\tau)=\int_{-\infty}^{+\infty}g(t)g(t+\tau)\mathrm{d}t$ is the correlation function of $g(t)$ whose Fourier transform is

$$\begin{aligned}\Phi_{gg}(f)&=\int_{-\infty}^{+\infty}\phi_{gg}(\tau)\mathrm{e}^{-\mathrm{j}2\pi f\tau}\mathrm{d}\tau\\&=\left[\int_{-\infty}^{+\infty}g(t)\mathrm{e}^{-\mathrm{j}2\pi f t}\mathrm{d}t\right]^2=|G(f)|^2.\end{aligned} \quad (6)$$

With $g(t)$ as a pulse with rectangular power spectrum expressed as

$$|G(f)|^2=\begin{cases}T_\mathrm{s}^2/2 & 0\leqslant|f|\leqslant 1/T_\mathrm{s}\\0 & |f|\geqslant 1/T_\mathrm{s}\end{cases}, \quad (7)$$

the inverse Fourier transform of (7) results in

$$\phi_{gg}(\tau)=T_\mathrm{s}\frac{\sin(2\pi\tau/T_\mathrm{s})}{2\pi\tau/T_\mathrm{s}}. \quad (8)$$

The output optical intensity $I_{\rm o}$ of the cascaded combination of DD-MZM and IM is expressed as

$$I_{\rm o}=\frac{1}{8}E_{\rm c}^2\Big[1+J_0(2\beta)+2\sum_{n=1}^{\infty}J_{2n}(2\beta)\cos(2n\omega t)\Big]\Big\{1+\cos\Big[\pi\frac{V_b}{V_\pi}+\pi\frac{v(t)}{V_\pi}\Big]\Big\},\tag{9}$$

where $V_{\rm b}$, V_π, and $v(t)$ are the DC bias voltage, the half-wave voltage, and the modulating signal voltage of IM, respectively.

By setting $V_{\rm b}=-V_\pi/2$, the modulation curve is

$$I_{\rm o}=\frac{1}{8}E_{\rm c}^2\Big\{1+J_0(2\beta)+2\sum_{n=1}^{\infty}J_{2n}(2\beta)\cos(2n\omega_s t)\Big\}\Big\{1+\sin\Big[\pi\frac{v(t)}{V_\pi}\Big]\Big\}\propto P_0\Big[1+\frac{2}{1+J_0(2\beta)}\sum_{n=1}^{\infty}J_{2n}(2\beta)\cos(2n\omega_s t)\Big]\Big\{1+\sin\Big[\pi\frac{v(t)}{V_\pi}\Big]\Big\},$$

where $P_0\propto E_c^2[1+J_0(2\beta)]/8$ is the DC part of the output optical power of IM. The AC part is related to the transfer function of IM. The 8th harmonic output in BS after O/E conversion provides the transfer function of IM and PD cascade as

$$T(v)=\frac{2RP_0J_8(2\beta)}{1+J_0(2\beta)}\sin\Big[\pi\frac{v(t)}{V_\pi}\Big],\tag{10}$$

where R is the PD responsivity.

Being an odd symmetric function, $T(v)$ can be expressed in a power series containing only odd order terms. The IM output contains non-linear distortion like clipping, as shown in Fig. 4.

Since the OFDM signal $v(t)$ is a sum of independent uniformly-distributed stochastic processes, if the total number of sub-carriers is larger than 10, $v(t)$ approximates a Gaussian process regardless of the statistical property of the individual information-bearing sub-carrier according to the central limit theorem, so that the output intensity of IM can be regarded as a non-linear transformation of the Gaussian process. Therefore, the auto-correlation function of the output intensity of IM can be expressed in a power series as

$$R_o(\tau)=\sum_{j=0}^{\infty}\frac{1}{j!}h_j^2\left[\frac{\overline{R_v(\tau)}}{\overline{R_v(0)}}\right]^j,\tag{11}$$

where the coefficient h_j is related with the transfer function $T(v)$ in an integration as

$$h_j=\frac{1}{\sqrt{\sum\limits_k\sigma_k^2}}\int_{-\infty}^{+\infty}T(v)H_j\Big(\frac{v}{\sqrt{\sum\limits_k\sigma_k^2}}\Big)\frac{1}{\sqrt{2\pi}}\exp\Big(-\frac{v^2}{2\sum\limits_k\sigma_k^2}\Big)\mathrm{d}v,\tag{12}$$

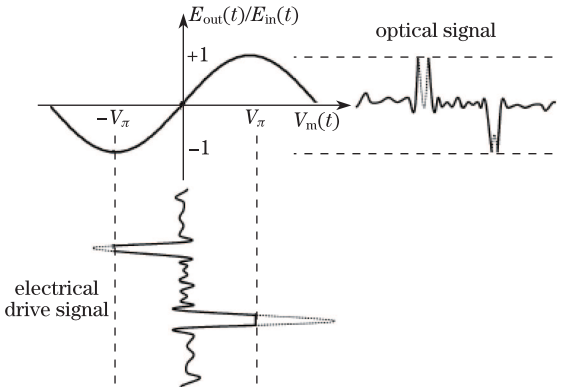

Fig. 4. Clipping of the OFDM signal caused by $LiNbO_3$ IM.

where $H_j(x)$ is the jth order Hermite polynomial.

The root mean square (RMS) value of optical modulation index for a single sub-carrier is defined as

$$\mu_k=\frac{\pi}{V_\pi}\sqrt{E\Big\{\frac{1}{2}A_k^2\Big\}}=\frac{\pi}{V_\pi}\sigma_k,\tag{13}$$

while the mean square modulation index for N sub-carriers is

$$\mu^2=\sum_{k=1}^{N}\mu_k^2=\Big(\frac{\pi}{V_\pi}\Big)^2\sum_{k=1}^{N}E\Big\{\frac{1}{2}A_k^2\Big\}=\Big(\frac{\pi}{V_\pi}\Big)^2\sum_{k=1}^{N}\sigma_k^2=\Big(\frac{\pi}{V_\pi}\Big)^2\sigma^2,\tag{14}$$

where $\sigma^2=\sum\limits_{k=1}^{N}\sigma_k^2$ represents the total average power of the OFDM sub-carriers.

Substituting Eq. (10) for $T(v)$ in Eq. (12) and carrying out the integration gives

$$h_{2j+1}=\frac{2RP_0J_8(2\beta)}{1+J_0(2\beta)}(-1)^j\mu^{2j+1}\mathrm{e}^{-\frac{1}{2}\mu^2}\quad j=0,1,2,3\cdots,\tag{15}$$

$$h_{2j}=0\quad j=0,1,2,3\cdots.\tag{16}$$

The auto-correlation function $R_{\rm o}(\tau)$ contains odd-order distortion terms which are as

$$\begin{aligned}R_{\rm o}(\tau)&=h_0^2+h_1^2\left[\frac{\overline{R_v(\tau)}}{\sigma^2}\right]+\frac{1}{3!}h_3^2\left[\frac{\overline{R_v(\tau)}}{\sigma^2}\right]^3+\frac{1}{5!}h_5^2\left[\frac{\overline{R_v(\tau)}}{\sigma^2}\right]^5+\cdots\\&=h_0^2+\frac{h_1^2}{\sigma^2}\left[\frac{1}{T_{\rm s}}\sum_{k=1}^{N}\sigma_k^2\phi_{gg}(\tau)\mathrm{e}^{\mathrm{j}(\omega_0+2\pi kf_{\rm s})\tau}\right]+\frac{1}{6}\frac{h_3^2}{\sigma^6}\left[\frac{1}{T_{\rm s}}\sum_{k=1}^{N}\sigma_k^2\phi_{gg}(\tau)\mathrm{e}^{\mathrm{j}(\omega_0+2\pi kf_{\rm s})\tau}\right]^3+\cdots.\end{aligned}\tag{17}$$

By substituting Eq. (8) for $\phi_{gg}(\tau)$ in Eq. (17) and taking the Fourier transform, the power spectrum of the

PD output is obtained as

$$S_{\rm o}(f) = \Big[\frac{2RP_0J_8(2\beta)}{1+J_0(2\beta)}\Big]^2\frac{\mu^2}{\sigma^2}{\rm e}^{-\mu^2}\frac{1}{T_{\rm s}}\sum_{k=1}^{N}\sigma_k^2 \cdot|G(f-f_0-kf_{\rm s})|^2 + \frac{1}{6}\Big[\frac{2RP_0J_8(2\beta)}{1+J_0(2\beta)}\Big]^2\frac{\mu^6}{\sigma^6}{\rm e}^{-\mu^2} \cdot\Big\{\frac{1}{T_{\rm s}}\sum_{k=1}^{N}\sigma_k^2\,|G(f-f_0-kf_{\rm s})|^2\otimes\frac{1}{T_{\rm s}}\sum_{k=1}^{N}\sigma_k^2 \cdot|G(f-f_0-kf_{\rm s})|^2\otimes\frac{1}{T_{\rm s}}\sum_{k=1}^{N}\sigma_k^2 \cdot|G(f-f_0-kf_{\rm s})|^2\Big\}, \tag{18}$$

where the first term represents the OFDM signal and the second term relates with the third distortion products. The triple beat products occur at frequencies $f_0+(\pm j\pm k\pm l)f_{\rm s}$. After gathering all triple beat products at the same sub-carrier frequency $f_0+kf_{\rm s}$ and counting the number of composite triple beat (CTB) products as C_{3k}, we obtain the following for the kth sub-band:

$$\begin{aligned}{\rm CTB}_k =& [(\text{Average Power of Composite Triple Beat Poducts})/(\text{Average Power of Sub-carrier})]_{{\rm at}\,f_0+kf_{\rm s}}\\ =& \frac{\frac{1}{6}[\frac{2RP_0J_8(2\beta)}{1+J_0(2\beta)}]^2\frac{\mu^6}{\sigma^6}\sigma_k^6{\rm e}^{-\mu^2}C_{3k}}{[\frac{2RP_0J_8(2\beta)}{1+J_0(2\beta)}]^2\frac{\mu^2}{\sigma^2}\sigma_k^2{\rm e}^{-\mu^2}} = \frac{1}{6}\frac{\mu^4\sigma_k^4}{\sigma^4}C_{3k}.\end{aligned} \tag{19}$$

When $\sigma_1^2=\sigma_2^2=\sigma_3^2=\cdots=\sigma_N^2$, $\sigma^2=N\sigma_1^2$, we have

$${\rm CTB}_k = \frac{\mu^4}{6N^2}C_{3k} = \frac{1}{6}\mu_1^4C_{3k}. \tag{20}$$

When the N sub-carriers fully occupy a frequency band and $N\gg1$, the frequency distribution of C_{3k} occurs at the band center with $C_{3k,\max}\approx 3N^2/8$, where the system performance will be identified as the worst case.

The CTB products of sub-carriers behave as the interfering noise which enhances the noise floor of receiver and in turn, affects the BER performance of the OFDM demodulator. Hence, the conventional formula for the bit error probability in a MQAM-OFDM system can be expanded to include the impact of the interference noise generated in IM and amplified in BS, which is written as

$$P_M \approx \frac{2}{\log_2 M}\Big(1-\frac{1}{\sqrt{M}}\Big)\times{\rm erfc}\left[\sqrt{\frac{3}{2(M-1)}\times\frac{1}{{\rm EVM}^2}}\right], \tag{21}$$

where EVM is the error vector magnitude. Meanwhile, EVM^2 is determined not only by the signal-to-white-noise ratio (SNR) but also by CTB as

$$\begin{aligned}{\rm EVM}^2 =& \frac{1}{\rm SNR}+\frac{1}{6}\frac{\mu^4\sigma_k^4}{\sigma^4}C_{3k}\\ =& \frac{N_0f_{\rm s}}{[\frac{2RP_0J_8(2\beta)}{1+J_0(2\beta)}]^2\frac{\mu^2}{\sigma^2}\sigma_k^2{\rm e}^{-\mu^2}G}+\frac{1}{6}\frac{\mu^4\sigma_k^4}{\sigma^4}C_{3k},\end{aligned} \tag{22}$$

where G is the overall RF gain in BS and N_0 is the output white noise spectrum density containing three components: thermal noise at the RF front of the optical receiver, the shot noise in the O/E conversion, and the laser relative intensity noise, which is expressed as

$$N_0 = \Big[\frac{4kT}{R_{\rm N}}+2{\rm e}RP_0+(RP_0)^2{10}^{0.1\times{\rm RIN}}\Big]GF \tag{23}$$

where k is the Boltzman's constant, T is the absolute temperature, $R_{\rm N}$ is the equivalent noise resistance, e is the electron charge, P_0 is the average received optical power, R is the PD responsivity, RIN is the relative intensity noise index of the laser, and F is the equivalent noise figure.

If $\sigma_1^2=\sigma_2^2=\sigma_3^2=\cdots=\sigma_N^2$, $\sigma^2=N\sigma_k^2$, then Eq. (22) is simplified to

$${\rm EVM}^2 = \frac{N_0f_{\rm s}}{[\frac{2RP_0J_8(2\beta)}{1+J_0(2\beta)}]^2\mu_1^2{\rm e}^{-N\mu_1^2}G}+\frac{1}{6}\mu_1^4C_{3k}. \tag{24}$$

The relationship between EVM^2 and μ_1 is composed of the SNR ratio term that is inversely proportional to μ_1^2 and the triple beat term that is proportional to μ_1^4. By setting the derivative of Eq. (24) with respect to μ_1^2 as 0, we find that the optimal value of μ_1^2 is

$$\mu_{1{\rm opt}}^2 \approx \sqrt[3]{\frac{3N_0f_{\rm s}}{[\frac{2RP_0J_8(2\beta)}{1+J_0(2\beta)}]^2GC_{3k}}}. \tag{25}$$

Substituting Eq. (25) for μ_1^2 in Eq. (24) gives the achievable minimum EVM^2 as

$${\rm EVM}^2_{\min} \approx \frac{1}{2}\sqrt[3]{\frac{(3N_0f_{\rm s})^2}{[\frac{2RP_0J_8(2\beta)}{1+J_0(2\beta)}]^4G^2}}C_{3k}^{1/3}. \tag{26}$$

Therefore, from Eqs. (21) to (26) and $C_{3k,\max}\approx 3N^2/8$, the BER and EVM systems are relative to the received optical power P_0, the white noise power spectrum N_0, the optical modulation index of each sub-carrier μ_1, and the sub-carrier number N.

A computation example is as follows. In a 40-GHz RoF system, such as in Fig. 3, consider $J_8(2\beta)=0.3244$ for the maximal 8th order harmonic generation. An optical power P_0=−2 dBm is received by PD in BS with responsivity R=0.7 mA/mW. The generated millimeter waves are a 40.040-GHz carrier and an OFDM-modulated lower side-band at 37.598 GHz. By looping back from point H to point O through an appropriate attenuator, the mixer output at point Q is the OFDM-modulated 2.442-GHz signal. The calculation results in $N_0=6\times10^{-19}{\rm A}^2/{\rm Hz}$ at $R_N=300\,\Omega$, F=2.47, G=23.5 dB, and RIN = −145 dB/Hz. The bandwidth of the OFDM signal is 100 MHz. For the effective sub-carriers, N=61 was selected out of the total number of 64, while the largest triple beat number is $C_{3k,\max}$=1 350. The symbol frequency is $f_{\rm s}=100/64=1.562\,5$MHz. An optimal μ_1 for the maximum signal to noise plus triple beat power ratio is found to be 2%. The curves of EVM^2 versus μ_1 are shown in Fig. 5 for different white noise powers. Each curve has a minimum value at the optimal μ_1. Below this value, EVM^2 increases due to lower SNR, whereas above this value, EVM^2 decreases due to signal distortion in IM.

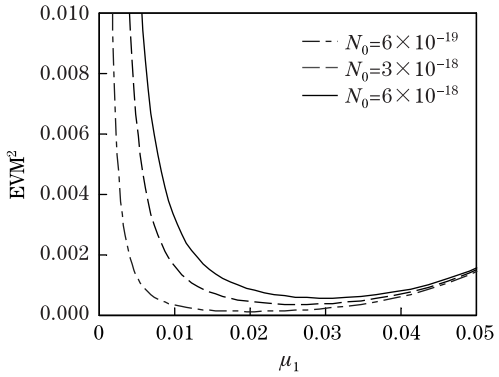

Fig. 5. EVM^2 versus μ_1 for different white noise powers.

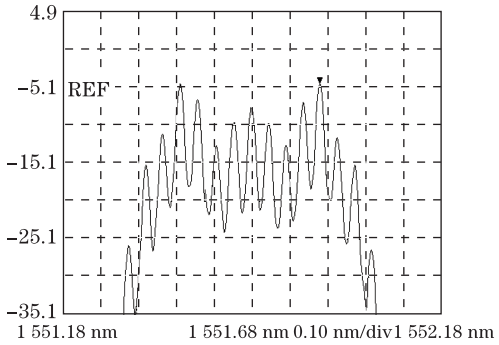

Fig. 6. Optical spectrum in the DD-MZM output for dual arms driven by 27-dBm RF signals.

5 Experiment of bi-directional RoF system based on OFM

The experiments are carried out not only for mm-generation, but also for OFDM modulation and two-way transmission. The RoF system shown in Fig. 3 is implemented.

Figure 6 shows the optical spectrum at the DD-MZM output port B in CS. When 5.005 GHz driving power reaches 27 dBm in the optical spectrum, several pairs of side-modes occur around the laser wavelength, among which the 4th ones, become the highest. The even symmetry of side-modes is necessary for generating millimeterwaves at frequencies $2n\times5.005$ GHz. Figure 7 shows the spectrum of the generated harmonics at point F in BS, among which is the 8th harmonic (n=4) as the highest. The spectrum of the OFDM-modulated 37.598 GHz lower side-band signal is shown in Fig. 8, which is

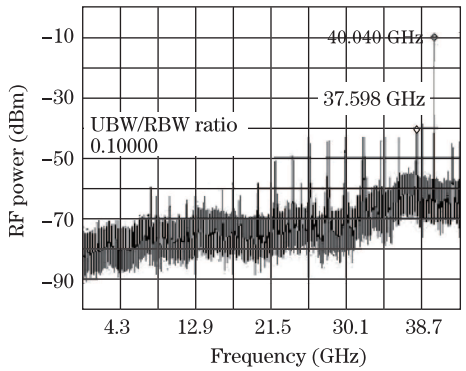

Fig. 7. RF spectrum of the PD output at point F.

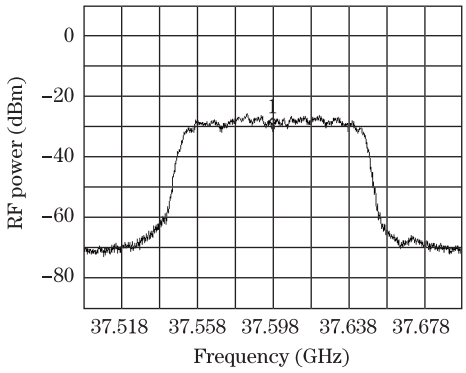

Fig. 8. RF spectrum of 37.6-GHz OFDM signal at point F.

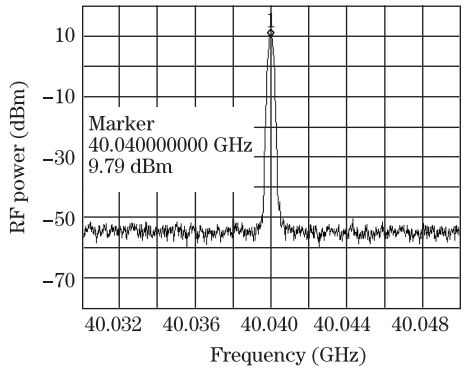

Fig. 9. RF spectrum of the amplified LO at 40 GHz in point G.

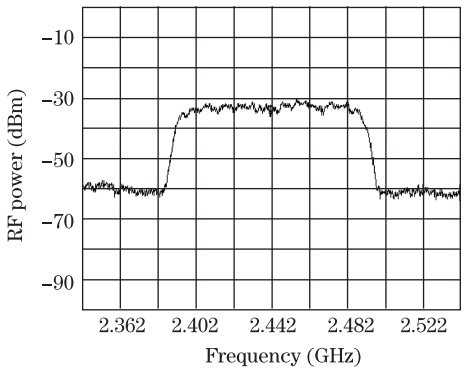

Fig. 10. RF spectrum of recovered 2.4-GHz OFDM at Rx.

filtered and amplified for transmission in the air. Figure 9 shows the 40.040-GHz pure carrier at point G in BS, coming from an extremely narrow BPF and being amplified up to 10 dBm as LO. Figure 10 shows the RF spectrum of the down-converted 2.442 GHz OFDM signal at point Rx, which is transmitted back from BS to CS.

For various driving levels of the 2.442 GHz OFDM signal at point V in CS, the measured EVM^2 versus σ at Rx is shown in Fig. 11 which matches well with the theoretical result, indicating that the EVM^2 model of Eqs. (22)−(26) is correct. The optimal driving level of the IF OFDM signal is about 3 dBm. The best OFDM-modulated IF level corresponds to the optimal RMS μ which is 15.6% for a $LiNbO_3$ IM with V_π=6.5 V. Since the OFDM signal has 61 effective sub-carriers, the corresponding $\mu_{1\mathrm{opt}}$ for each sub-carrier is 2%.

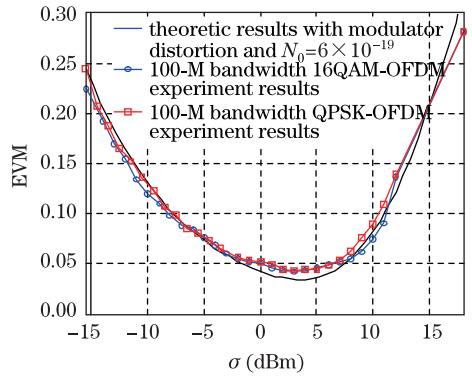

Fig. 11. EVM versus driving IF power to IM in CS.

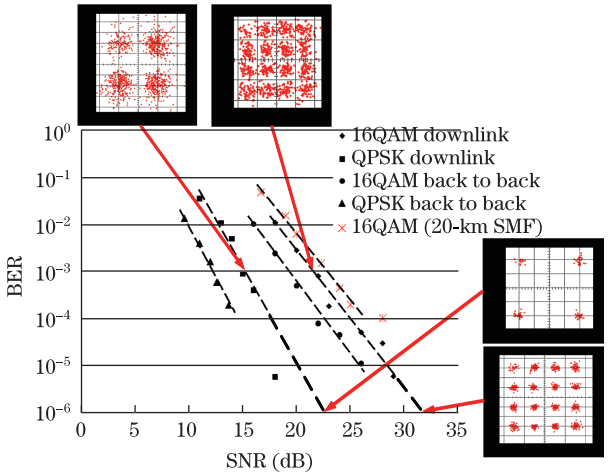

Fig. 12. BER versus output SNR at Rx.

BER versus the output SNR at point Rx in CS is shown in Fig. 12. For a given BER, the required SNR of the 16QAM scheme is 6–7 dB higher than that of the quadrature phase shift keying (QPSK) scheme. Compared with the base-band, back-to-back case the SNR degradation caused by RoF without an optical fiber is around 2 dB, whereas 20-km fiber causes 1 dB more SNR penalty. The signal constellations of QPSK and 16QAM are shown both at BER 10^{-3} and 10^{-6}. This experiment has been performed for the 64-point fast Fourier transform (FFT) OFDM signal at 1.5625 Msym/s symbol rate. Excluding 16 pilot tones, the effective number of sub-channels for the data transmission is 45, which determines the total bit rate that is up to 280 Mb/s for the 16QAM scheme.

After setting the best optical modulation index to IM for the OFDM IF signal and the received optical power (−2 dBm for BS and −8 dBm for CS), the real-time RoF/wireless transmission using 802.11n devices was performed. The recovered 16/64QAM constellations after 5-km fiber downlink measured in WT and the uplink at Rx in CS are shown in Figs. 13(a) and (b), respectively. The EVM of 16QAM or 64QAM-modulated OFDM signal is −24−−25 dB, a merit figure good enough for stable transmission. Thus, the bi-directional 100 Mb/s Ethernet data transmission between CS and WT is performed without packet loss.

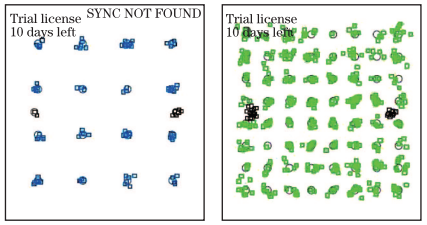

(a) 802.11n downlink constellation

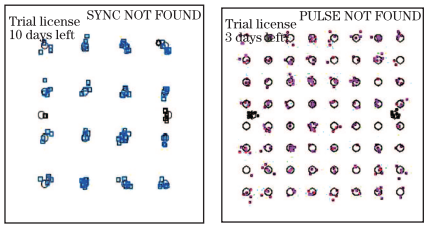

(b) 802.11n uplink constellation

Fig. 13. Recovered constellation of 16/64QAM.

6 Summary

A bi-directional 40-GHz RoF transmission platform based on OFM is designed and implemented using DD-MZM and other cost-effective devices. This OFM system is proven more cost-effective and stable than the original version using optical PM plus MZI. An OFDM IF signal modulates the light wave. A pure 40-GHz carrier is created as LO for down-converting the received OFDM-modulated millimeter wave into the IF signal to ease uplink optical transmission.

This work was supported by the National Natural Science Foundation of China (No. 60877053) and Shanghai Science and Technology Development Funds (No. 11511502500).

References

1. Ton Koonen, Anthony Ng'oma, Maria Garcia Larrocle *et al.*. Novel cost-effective techniques for microwave signal delivery in fiber-wireless networks [C]. In (Ed.), Proc. ECOC2004, Stockholm, Sweden, 120∼123
2. M. G. Larrod**é**, A. M. J Koonen, J. J. V Olmos *et al.*. Dispersion tolerant radio-over-fiber transmission of 16 and 64-QAM radio signals at 40GHz [J]. *Electron. Lett.*, 2006, **42**(15): 872∼874
3. H. Yang, J. Zeng, Y. Zheng *et al.*. Evaluation of Effect of MZM Nonlinearity on QAM and OFDM Signals in RoF Transmitter [C]. Microwave Photonics Conference, 2008, jointly held with the 2008 Asia-Pacific Microwave Photonics Conference, MWP/APMP 2008, Sept. 9-Oct. **3**, 2008, 90∼93
4. Chun-Ting Lin, Jyehong Chen, Po-Tsung Shih *et al.*. Ultra-High Data-Rate 60 GHz Radio-Over-Fiber Systems Employing Optical Frequency Multiplication and OFDM Formats [J]. *J. Lightwave Technology*, 2010, **28**(16): 2296∼2306
5. Yi Li, Rujian Lin, Yingchun Li. Bi-directional mm-Wave Radio-over-Fiber System Based on OFM and Modulated by OFDM [C]. 2009 IET International Communication Conference on Wireless Mobile & Computing Proceedings, Dec.7-9, 2009, Shanghai, China, 13∼16

6. Xiang Liu, Fred Buchali, Robert W. Tkach. Improving the Nonlinear Tolerance of Polarization-Division-Multiplexing CO-OFDM in Long-Haul Fiber Transmission [J]. *J. Lightwave Technology*, 2009, **27**(16): 3632∼3640
7. Lin Ru-Jian, Chen Rong, Liu Xie-Hua. Laser Clipping Effect on CSO and CTB in AM-VSB Lightwave CATV Systems [C]. IOOC'95, Technical Digest, FC2-4,78∼79
8. Daniel J. Fernandes Barros and Joseph M. Kahn, Optical Modulator Optimization for Orthogonal Frequency-Division Multiplexing [J]. *J. Lightwave Technology*, 2009, **27**(13): 2370∼2378